Biomacromolecules

ACS Editors' Choice

Article

pubs.acs.org/Biomac

Terms of Use

Microfluidics-Assisted Fabrication of Gelatin-Silica Core−Shell Microgels for Injectable Tissue Constructs

Chaenyung Cha,[†,‡] Jonghyun Oh,[†,§] Keekyoung Kim,[∥] Yiling Qiu,[⊥] Maria Joh,[‡] Su Ryon Shin,[‡,○] Xin Wang,[#] Gulden Camci-Unal,[‡] Kai-tak Wan,[#] Ronglih Liao,[⊥] and Ali Khademhosseini*[,‡,○]

[‡]Harvard-MIT Division of Health Sciences and Technology, Division of Biomedical Engineering, Department of Medicine, Brigham and Women's Hospital, Harvard Medical School, Cambridge, Massachusetts 02139, United States

[§]Division of Mechanical Design Engineering, Chonbuk National University, Jeonju 561-756, South Korea

[∥]School of Engineering, University of British Columbia, Kelowna, British Columbia V1V 1V7, Canada

[⊥]Division of Cardiology and Division of Genetics, Department of Medicine, Brigham and Women's Hospital, Harvard Medical School, Boston, Massachusetts 02115, United States

[#]Department of Mechanical and Industrial Engineering, Northeastern University, Boston, Massachusetts 02115, United States

[○]Wyss Institute for Biologically Inspired Engineering, Harvard University, Boston, Massachusetts 02115, United States

Supporting Information

ABSTRACT: Microfabrication technology provides a highly versatile platform for engineering hydrogels used in biomedical applications with high-resolution control and injectability. Herein, we present a strategy of microfluidics-assisted fabrication photo-cross-linkable gelatin microgels, coupled with providing protective silica hydrogel layer on the microgel surface to ultimately generate gelatin-silica core−shell microgels for applications as in vitro cell culture platform and injectable tissue constructs. A microfluidic device having flow-focusing channel geometry was utilized to generate droplets containing methacrylated gelatin (GelMA), followed by a photo-cross-linking step to synthesize GelMA microgels. The size of the microgels could easily be controlled by varying the ratio of flow rates of aqueous and oil phases. Then, the GelMA microgels were used as in vitro cell culture platform to grow cardiac side population cells on the microgel surface. The cells readily adhered on the microgel surface and proliferated over time while maintaining high viability (~90%). The cells on the microgels were also able to migrate to their surrounding area. In addition, the microgels eventually degraded over time. These results demonstrate that cell-seeded GelMA microgels have a great potential as injectable tissue constructs. Furthermore, we demonstrated that coating the cells on GelMA microgels with biocompatible and biodegradable silica hydrogels via sol−gel method provided significant protection against oxidative stress which is often encountered during and after injection into host tissues, and detrimental to the cells. Overall, the microfluidic approach to generate cell-adhesive microgel core, coupled with silica hydrogels as a protective shell, will be highly useful as a cell culture platform to generate a wide range of injectable tissue constructs.

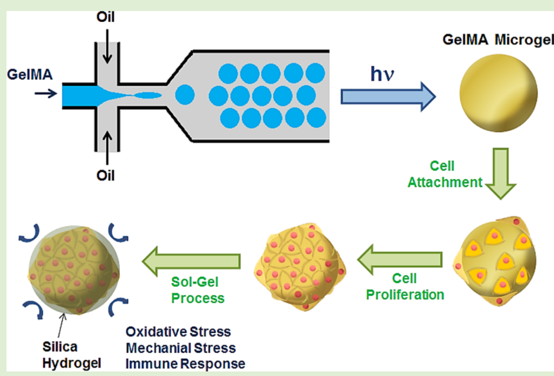

■ INTRODUCTION

Hydrogels are widely used as a scaffold material for tissue engineering applications. The hydrophilic and biocompatible polymer networks of hydrogels can closely mimic native extracellular matrices (ECM) and provide suitable microenvironments for cells by controlling their mechanical and biomolecular transport properties.[1−3] Furthermore, hydrogels can be intelligently designed to present functional moieties (e.g., cell adhesion and degradation domains and growth factors) that can transmit signals to surrounding cells for desired behavior.[4,5]

More recently, microfabrication techniques are being utilized to engineer hydrogels in micrometer dimensions, with the goal of achieving high-resolution control and miniaturization for cost-effective and high-throughput experiments, and engineering injectable constructs.[6,7] Microfluidics has emerged as one such technology that allows the fabrication of microscale hydrogels ("microgels") in a highly efficient, controllable, and scalable manner.[8,9] The microfluidic devices generally consist of coaxial flow or flow-focusing channels that allow for the formation of uniform-sized aqueous emulsion particles (i.e., droplets) dispersed within an oil phase.[8−10] The droplets containing gel-forming molecules are generated from the microfluidic device, followed by a polymerization reaction to fabricate the microgels.

Received: October 16, 2013
Revised: December 10, 2013
Published: December 17, 2013

Here, we utilized a microfluidic flow-focusing device to fabricate methacrylated gelatin (GelMA) microgels with a high degree of controllability in size. In addition, we further engineered the GelMA microgels by providing a layer of silica hydrogel "shell" in order to protect the cells cultured on GelMA microgels from harmful external environment such as oxidative stress during injection and implantation.[11,12] These gelatin-silica core−shell microgels would ultimately serve as a highly versatile platform for in vitro cell culture and injectable tissue constructs. GelMA hydrogels have been successfully demonstrated as tissue engineering scaffolds in several previous applications.[13−16] GelMA presents multiple methacrylic groups on a gelatin molecule, which allows for the hydrogel formation via radical polymerization. Therefore, GelMA droplets containing photo-initiator, generated from the microfluidic device, could be photopolymerized in situ by exposure to UV light to produce GelMA microgels in an efficient manner. The microfluidic approach also allows for a precise control of microgel size by tuning the flow rates of GelMA solution and oil phase. Then, GelMA microgels were used as an in vitro platform to culture cardiac cells on their surfaces.

In this work, cardiac side population (CSP) cells were cultured on the surface of GelMA microgels, and their viability and proliferation were evaluated. CSP cells have gained recognition in recent years for their role in cardiac regeneration, as they are progenitor cells shown to undergo cardiomyogenic differentiation in various in vitro and in vivo studies.[17,18] In addition, the migration of CSP cells seeded on GelMA microgels to a cell-adhesive environment was monitored to evaluate the potential of cell-seeded microgels as injectable cardiac tissues. Furthermore, a strategy of providing a protective shell was employed by coating the cell-seeded microgels with silica hydrogels, and its protective capacity against external environment was evaluated by exposing them to induced oxidative stress. We also monitored the biodegradation of silica hydrogel shell over time, and evaluated the bioactivity of the CSP cells underneath the silica hydrogel by measuring their viability and evaluating their capacity for migration and proliferation.

■ MATERIALS AND METHODS

Synthesis of Methacrylated Gelatin (GelMA). To conjugate methacrylate functional groups on gelatin molecules, 5 g of gelatin (Sigma Aldrich) and 0.5 g of 4-(dimethylamino)-pyridine (Sigma Aldrich) were first dissolved in dimethyl sulfoxide at 50 °C. Then, 2 mL of glycidyl methacrylate (Sigma Aldrich) was slowly added to the mixture, which was continuously stirred at 50 °C for two days under dry N_2 gas. The mixture was dialyzed against deionized (DI) water for 3 days, while changing the DI water twice a day. The product was obtained by lyophilization. The presence of methacrylate groups on gelatin was confirmed with ^{1}H NMR (Figure S1 in Supporting Information).

Fabrication of Microfluidic Flow-Focusing Device. The silicon master, which would be served as a template for polydimethysiloxane (PDMS)-based microfluidic device, was fabricated on a silicon wafer using a standard photolithography technique.[19,20] Briefly, SU-8 2000 (MicroChem Corp.) as a photoresist was first spin-coated on a silicon wafer and then baked at 95 °C to remove the solvent and harden the photoresist. A photomask with patterns for the microfluidic channels was placed on top of the wafer, and exposed to UV to cross-link the patterned area. After baking at 95 °C to further solidify the cross-linked photoresist, the wafer was cooled to room temperature, and placed in SU-8 developer to remove the unexposed photoresist. The wafer was then rinsed with isopropanol three times and dried. The schematic illustration of the silicon master is shown in the Supporting Information (Figure S2).

PDMS was fabricated on top of the silicon master by placing the mixture of silicone elastomer base and the curing agent (10:1 mass ratio, Sylgard184 Silicone Elastomer Kit) on the master. It was placed under vacuum to remove bubbles, and cured at 80 °C for 3 h. After detaching the PDMS from the master, the holes for fluid inlets and outlets (0.5 mm diameter) were punched out. The PDMS substrate and a glass slide were exposed to oxygen plasma (Harrick Plasma) for 1 min and then irreversibly bonded to each other to fabricate the PDMS microfluidic device.

Fabrication of GelMA Microgels. Figure 1a shows the schematic description of droplet generation by microfluidic flow-focusing channels. The aqueous phase (8 wt % GelMA and 0.2 wt % Irgacure 2959 in phosphate buffered saline (PBS, pH 7.4)) and the oil phase (20 wt % Span80 in mineral oil) are injected into the inlets of the microfluidic device from syringes (BD Biosciences) connected by plastic tubing (0.3 mm inner diameter and 0.76 mm outer diameter). The fluid injection and flow rates were controlled by syringe pumps (PHD 2000, Harvard Apparatus). The experimental setup was placed on top of the sample stage of an inverted optical microscope (Eclipse TE2000-U, Nikon) to monitor the droplet formation.

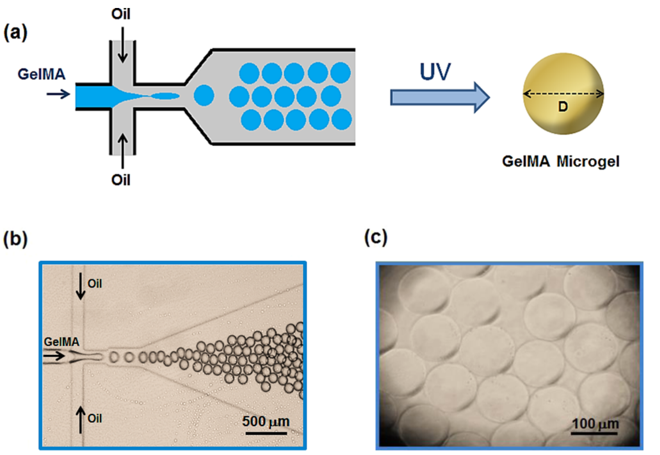

Figure 1. (a) Microfluidic fabrication of GelMA microgels. Aqueous droplets made of GelMA pregel solution, generated from a microfluidic flow-focusing device, were photopolymerized to form GelMA microgels. (b, c) Microscopic images of a microfluidic flow-focusing device generating GelMA droplets (b) and GelMA microgels fabricated by UV-initiated photopolymerization of GelMA droplets (c).

The droplets, exiting from the outlet and passing through the connected plastic tubing (0.3 mm inner diameter and 0.76 mm outer diameter), were irradiated with UV light for 5 min (Series 2000, OmniCure) to photopolymerize the droplets. The intensity of UV was 850 mW, and the distance between the light source and the tubing was 8 cm. The fabricated microgels were collected into each microtube (1.5 mL, Eppendorf) containing 1 mL of PBS for 20 min and then centrifuged to remove the oil phase. The microgels were washed with PBS three times. The experiments were performed at room temperature.

Evaluation of Elasticity of GelMA Microgels with Nano-indentation. Force measurements on GelMA microgels were performed using atomic force microscopy (AFM)-assisted nano-indentation, as previously described.[21] Briefly, the experimental setup consisted of the AFM (Agilent 5500) placed on top of an inverted optical microscope, which allowed monitoring of the AFM cantilever and the microgel sample during indentation measurement. The spring constant of the cantilever, measured using Cleveland method, was 0.20 N m^{-1}.[22] The cantilever was initially positioned at the center of the microgel, and then lowered at the rate of 3 μm s^{-1} to indent the microgel. The applied force (F) was measured as a function of the position of the cantilever. The elastic modulus (E) was calculated using Hertz contact mechanics theory for the spherical elastic solid:[23]

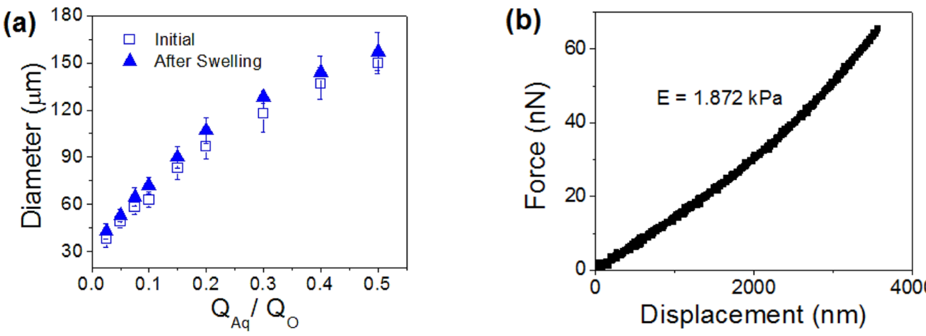

Figure 2. (a) Diameter of GelMA microgels (8 wt %), before and after swelling in PBS, was controlled by the ratio of flow rates of aqueous phase (GelMA pregel solution) to oil phase (Q_{Aq}/Q_O). (b) Force-displacement curve of a GelMA microgel measured by an AFM-assisted nanoindentation. Elastic modulus (E) was calculated using Hertz contact mechanics theory (eq 1).

$$F = \frac{4}{3}\left(\frac{E}{1-\nu^2}\right)R^{1/2}h^{3/2} \tag{1}$$

where R is the radius of the microgel sphere, h is the indentation depth, and ν is the Poisson's ratio of GelMA microgel and equals to 0.5, assuming the hydrogel follows the ideal rubber. To validate the results, cylindrical GelMA hydrogels at the same concentration (8 wt %) were prepared as previously described.[13] Then, the hydrogels were compressed uniaxially, and the strain−stress curves were obtained using a mechanical testing unit (Model 5943, Instron). Elastic modulus was calculated as the slope of initial linear region (10% strain) of a stress−strain curve.

Fabrication of Silica Hydrogel Shell. Silica hydrogel was fabricated by a sol−gel method.[12] Silica sol was first generated by adding 20 μL of HCl (1 M) to 1 mL of tetramethyl orthosilicate (50% (v/v), Sigma Aldrich), and stirred at room temperature for 30 min to initiate the polycondensation reaction. Then, 10 μL of the silica sol mixture was added to 1 mL of aqueous solution containing GelMA microgels (in PBS), and continuously stirred over time to fabricate silica gel on the microgel surface. At different time points, a small sample was taken and the thickness of the silica hydrogel coated on the microgel was measured using an inverted optical microscope (Eclipse Ti, Nikon).

Cell Culture on GelMA Microgels. CSP cells were isolated from C57BL6 mice (Charles River Laboratories) hearts. The detailed procedures of isolation and purification of the cells are provided elsewhere.[24] The isolated cells were cultured in cell growth media (Minimum Essential Medium Alpha (Lonza), supplemented with 20% fetal bovine serum (HyClone), 1% penicillin/streptomycin (Invitrogen), and 6 mM L-glutamine (Sigma Aldrich)).

CSP cells and GelMA microgels are mixed in the culture media containing GelMA microgels (100 microgels, 20000 cells per mL), and 2 mL of the mixture were placed in each well of a six-well plate (nontreated, BD Falcon). The cell−microgel mixture was incubated at 37 °C with 5% CO_2 with shaking at 50 rpm. The culture media was changed every three days. The cell adhesion to the microgels and proliferation were monitored with an inverted optical microscope (Eclipse Ti, Nikon). The number of cells was counted at various time points, and the proliferation rate (k_P) was calculated using the following equation:[25]

$$\frac{N_t}{N_0} = 2^{k_P t} \tag{2}$$

where N_t represents the number of cells at time, t, and N_0 represents the initial number of cells.

Oxidative Stress Test. The cell-seeded microgels with or without silica hydrogel shell were incubated in the culture media supplemented with 0.2 μM of hydrogen peroxide to generate reactive oxidative species.[26] After 1 h of incubation, the viability of cells on the microgels was evaluated using LIVE/DEAD Viability Kit (Invitrogen). Briefly, the cells were fluorescently labeled with calcein-AM (green) and ethidium homodimer-1 (red) to visualize the live and dead cells, respectively, using a fluorescence microscope (Observer D1, Zeiss). The numbers of live and dead cells were manually counted. The viability was reported as the percentage of the live cells from total cells.

Biodegradation of Silica Hydrogel. Degradation of silica hydrogel was evaluated by measuring the amount of degraded product, silicic acid, using the silicomolybdate method developed by Iler et al.[27,28] Briefly, the silica-coated microgels were incubated in PBS at 37 °C (100 microgels in 4 mL of culture media). At various time points, a small sample of the media (50 μL) was collected and incubated with 450 μL of molybdate reagent (0.4 wt % ammonium molybdate in 50 mM sulfuric acid) for 10 min to allow the formation of silicomolybdate complex which has a characteristic yellow color. Then, the absorbance of the silicomolybdate was monitored with UV−vis spectrophotometer (ND-1000, Thermo Fisher). The absorbance of pure PBS was used as a negative control. The plot of absorbance at 400 nm (A_{400}) versus time (t) was fitted with a first-order degradation kinetics model:[29,30]

$$A_{400} = A_0 \exp(k_D t) \tag{3}$$

where A_0 is the initial absorbance and k_D is the degradation rate (in day^{-1}).

RESULTS AND DISCUSSION

Microfluidic Fabrication of GelMA Microgels. Spherical microgels made of cross-linked gelatin were prepared by photopolymerization of GelMA droplets generated from a microfluidic flow-focusing device (Figure 1a,b, Video S1 in Supporting Information). The flow-focusing geometry of the microfluidic device is designed to generate aqueous droplets by the shear stress of oil phase. Here, the aqueous phase consisted of GelMA (8 wt %) and Irgacure2959 (0.2 wt %), so the droplets could be photopolymerized to form microgels (Figure 1c). The concentration of GelMA was chosen from a range which is above a lower critical concentration of hydrogel formation (4.5 wt %) and below a concentration that impedes stable droplet formation within microchannels due to its high viscosity (15 wt %; Figure S3 in Supporting Information).[13,31] The oil phase consisted of mineral oil supplemented with Span80 (20 wt %) as a surfactant to stabilize the droplets and increase the viscosity of the oil phase to generate sufficient shear stress for droplet generation. In addition, the presence of surfactants decreases the dynamic surface tension of the aqueous solution, leading to more efficient droplet formation during a rapid time frame. Pure mineral oil could not generate GelMA droplets because the viscosity of the mineral oil was not high enough to generate adequate shear stress (Figure S4a in Supporting Information). Similarly, droplets generated by the mineral oil supplemented with low concentration of Span80 (8 wt % in mineral oil) were not stable enough to maintain their spherical structure (Figure S4b in Supporting Information).

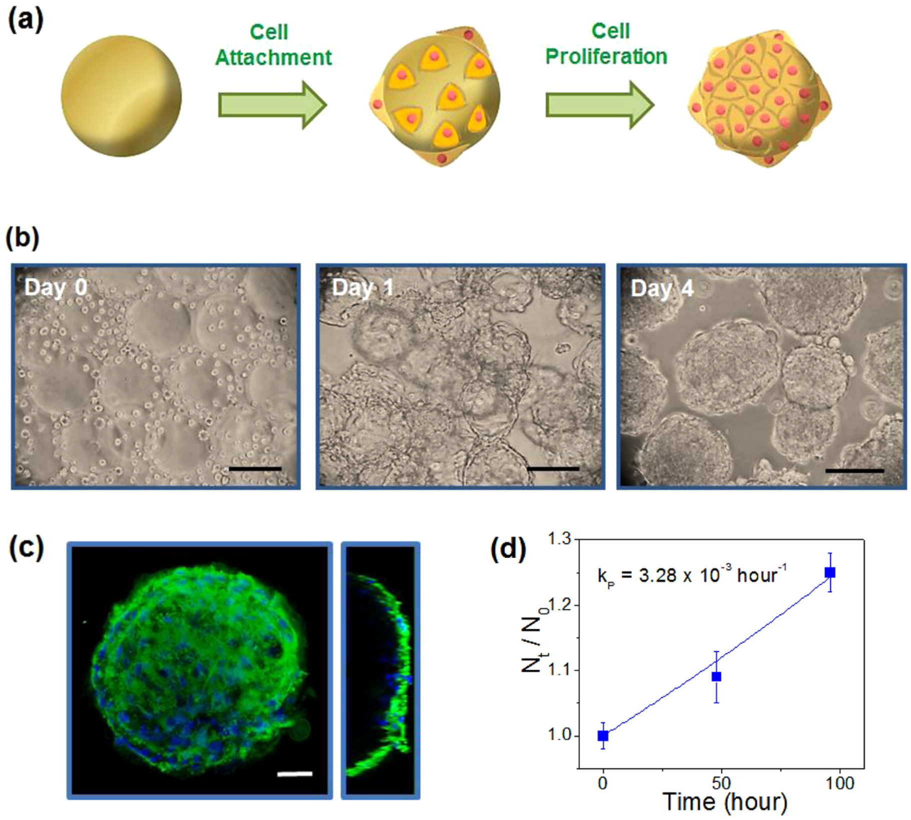

Figure 3. (a) GelMA microgels were used as in vitro platform to culture cells on the surface. (b) Microscopic images of CSP cells cultured on GelMA microgels. The cells adhered on the surface of GelMA microgels and proliferated over time (scale bar: 100 μm). (c) A confocal fluorescent microscopic image of CSP cells on GelMA microgel. The cells were stained with Alexa488-phalloidin and DAPI to visualize actin and nuclei, respectively (scale bar: 20 μm). A cross-sectional image is shown on the right panel. (d) The number of cells (N_t) at time, t, normalized with the initial number of cells (N_0) were plotted and fitted with eq 2 (k_P: proliferation rate).

Physical Properties of GelMA Microgels. One critical advantage of utilizing microfluidic flow-focusing channel over conventional emulsification methods using mechanical agitation (e.g., sonication) in making droplets is the ability to generate highly monodisperse droplets and efficient control their size.[10] In the flow-focusing microfluidic geometry, size of the droplets can be controlled by changing the shear stress applied to the aqueous flow.[32] This is typically accomplished by changing the ratio of the flow rates of aqueous and oil flows (Q_{Aq}/Q_O). To generate GelMA droplets with varying diameters, the flow rate of aqueous phase (Q_{Aq}) was kept constant at 4×10^{-12} m^3 s^{-1}, while changing the flow rate of oil phase (Q_O) from 8×10^{-12} m^3 s^{-1} to 8×10^{-11} m^3 s^{-1} in order to obtain a range of Q_{Aq}/Q_O from 0.05 to 0.5. The diameter of GelMA microgels changed from 35 to 150 μm (Figure 2a, Figure S5 in Supporting Information). When the microgels were incubated in PBS, there was a small increase in diameter due to swelling of the microgels.

The stiffness of the GelMA microgel was evaluated by calculating the elastic modulus from force-displacement curves, which was determined from AFM-assisted nanoindentation technique (Figure 2b, Figure S6 in Supporting Information). The elastic modulus, calculated using Hertz contact mechanics theory (eq 1), was 1.87 kPa (±0.23). To validate the modulus obtained from the nanoindentation, cylindrical GelMA hydrogel at the same concentration was prepared separately. The elastic modulus calculated from the stress−strain curve obtained with unconfined compression (2.23 ± 0.34 kPa) was in the same range of the modulus of spherical microgels by the nano-indentation. This proved that the microgels with controlled shapes and sizes could properly form under the reaction condition (i.e., photopolymerization of droplets dispersed in oil phase).

CSP Cell Adhesion on GelMA Microgels. Microgel-based cell culture platforms demonstrate several advantages over conventional tissue culture plates or flasks. To begin with, microgels have much greater surface-to-volume ratio, therefore more cells can be cultured with less substrate volume. Furthermore, hydrogels can easily be tuned to more closely mimic physiological conditions (e.g., rigidity and cell-responsive ligands) compared to hard plastic or glass surface. In addition, cell-seeded microgels can be utilized as injectable tissue constructs.

CSP cells were cultured on the GelMA microgels to study their adhesion behavior on the microgel surfaces in order to assess the suitability of GelMA microgels as in vitro cell culture platform (Figure 3a). The GelMA microgels with having the diameter of 100 μm were chosen for this study, as the microgels of this size provide enough surface area for multiple cells to adhere while retaining their injectability through needles. CSP cells are a class of progenitor cells that have been shown to undergo differentiation into functional cardiomyocytes, therefore, considered to be a highly promising cell source for cardiac regenerative therapies.[17,18] Thus, CSP-seeded GelMA microgels may potentially be used as injectable cardiac tissue constructs. First, CSP cells were suspended in culture media containing GelMA microgels. The mixture was continuously stirred during the culture to prevent the microgels from aggregation by the cells adhering to multiple microgels. After one day of culture, the cells

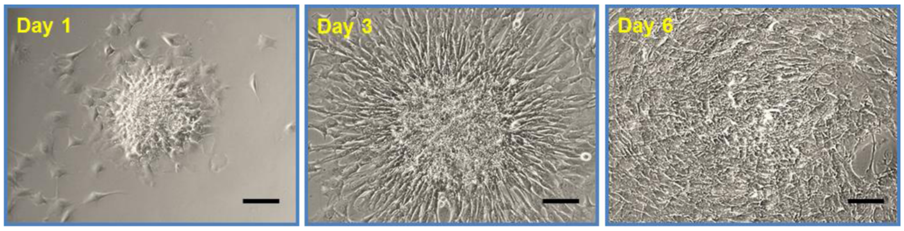

Figure 4. CSP cells on GelMA microgels were placed on a cell adhesive surface, and their adhesion and proliferation over time were monitored (scale bar: 50 μm).

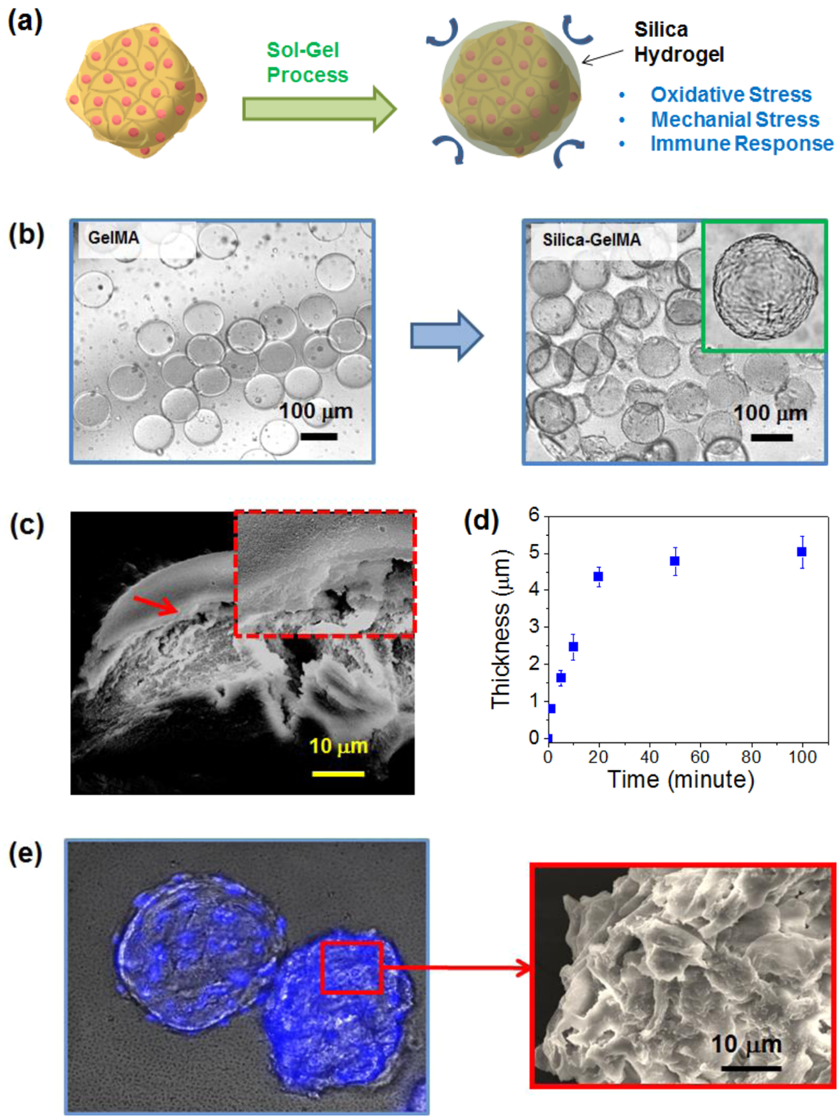

Figure 5. (a) Schematic description of fabrication of protective silica hydrogel shell on the GelMA microgels. (b) Optical microscopic images of GelMA microgels and silica-coated GelMA microgels. (c) The silica hydrogel was further characterized with scanning electron microscopy (SEM). Inset shows the magnified view of the silica hydrogel shell on top of GelMA microgel core, identified with an arrow. (d) The thickness of the silica hydrogel measured over the reaction time. (e) (Left) A microscopic image of CSP cells on GelMA microgels coated with silica gel. A fluorescent image of the cell nuclei stained with DAPI (blue) was overlaid to identify the cells. (Right) SEM image shows the surface of cells covered with silica hydrogel.

adhered and spread onto the surface of the microgels (Figure 3b,c). In addition, the cells on the microgels proliferated over time, as evidenced by the increase in the number of cells (Figure 3b,d, Figure S7 in Supporting Information). This result demonstrated that the GelMA microgels could be successfully used as an in vitro cell culture platform to provide a suitable microenvironment for CSP cells.

To evaluate whether the CSP cells adhered to the microgels could migrate and spread to other surrounding environment, a likely event after which the cells are transplanted to the target tissue, the cell-seeded microgels were placed on top of tissue-culture treated plastic surface, and monitored the cellular behavior. After one day, the cell-seeded microgels adhered on the surface, and the cells on the periphery began to migrate from

dx.doi.org/10.1021/bm401533y | *Biomacromolecules* 2014, 15, 283−290

the microgels to the plastic surface (Figure 4). These cells began to proliferate over time, covering the entire surface. Interestingly, the spherical structure of the microgels eventually disappeared over time likely due to the degradation induced by the cells.

It should be noted here that we have chosen to culture the cells on the microgel surface (2D approach) rather than encapsulate within the microgel (3D approach) for the following reasons, even though the 3D approach can more closely mimic the native environment: First, the cells can proliferate more quickly on the surface, and therefore a high number of cells could be efficiently obtained. On the other hand, the cell proliferation within the microgel is highly limited due to the confined inner space of the microgels. Second, it is easier to detach and collect the cells from the surface, whereas it becomes more difficult to isolate the encapsulated cells from the microgels. Third, since the cells must be included in the pregel solution and go through the microfluidic channels for encapsulation within the microgels, more stringent conditions for microfluidic droplet generation and gelation (e.g., temperature, flow rate, surfactant concentration, type of oil, and cross-linking step) must be applied in order to maintain the cell viability.

Silica Hydrogel Shell on GelMA Microgel Core. One of the major problems associated with cell transplantation therapy is the low viability of cells after transplantation, because the cells are exposed to external factors such as reactive oxidative species, host immune response, and mechanical stress during injection and after implantation.[33−35] To prevent these factors from adversely affecting the CSP cells on the microgels during injection or after implantation, a strategy of coating the cell-seeded microgel "core" with silica hydrogel as a protective "shell" was employed (Figure 5a). Silica hydrogel, prepared using sol−gel process, was chosen here as it offers several advantages.[11,12,36] First, the sol−gel process can be done in mild conditions; silica sol, which is a collection of silica macromers and colloids, can undergo sol−gel transition at physiological pH in which the macromers and colloids coalesce and further condense to form silica hydrogel, and also does not require potentially toxic cross-linking molecules and catalysts. In addition, the silica hydrogel has high mechanical durability and resistance to thermal and chemical denaturation.[37,38] Furthermore, the viability and metabolic activities of encapsulated cells have shown to be well maintained due to the diffusional properties of silica hydrogels.[39] Moreover, silica hydrogels undergo bioresorption process in living organisms, in which silica gel is dissolved in biological fluids and the degradation products are cleared from the body.[40,41] For these reasons, silica hydrogels prepared by sol−gel process have been extensively utilized in various biomedical applications, including drug delivery systems, bioreactors, biosensors, and cell encapsulation.[11,12,36]

Here, the sol−gel process to fabricate silica hydrogels was carried out on the surface of the GelMA microgels. The acid-catalyzed polycondensation of tetramethyl orthosilicate (50 wt % in water) to produce aqueous sol was first performed separately prior to the coating process. Then, a small amount of sol (0.5 wt %) was added to PBS containing GelMA microgels, after which the silica hydrogel began to form on the microgel surface. The accumulation of silica hydrogel on the microgel surface is driven by the surface hydroxyl groups which participate in the silica condensation.[36] Optical and scanning electron microscopic analyses confirmed that coating of silica hydrogel on top of GelMA microgels was successfully achieved (Figure 5b,c). The thickness of the silica hydrogel increased with increasing reaction time and leveled off in 30 min, indicating the completion of silica hydrogel formation (Figure 5d). The silica hydrogel was also successfully formed on the cell-seeded microgels, demonstrating that the presence of cells did not affect the gelling process of the silica (Figure 5e). In addition, silica hydrogel shell did not affect the viability of the cells, which further indicated that the process was biocompatible and the thickness of silica hydrogel did not hinder nutritional transport for the cells (Figure 6).

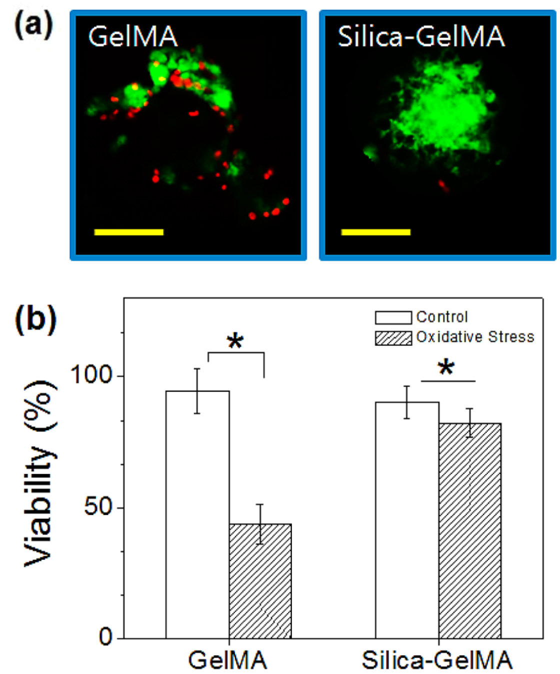

Figure 6. (a) Fluorescent images of CSP cells on GelMA microgels (left) and GelMA microgels coated with silica hydrogel (right), subjected to oxidative stress. The cells were stained with calcein-AM (green) and ethidium homodimer-1 (red) to visualize live and dead cells, respectively (scale bar: 50 μm). (b) Viability of the CSP cells was quantified as the percentage of the live cells (*$p < 0.05$).

In Vitro Oxidative Stress Test. To evaluate the protective capacity of the silica hydrogel shell on the CSP cells, the cell-seeded microgels with or without the silica hydrogel shell were exposed to oxidative stress environment (Figure 6). The oxidative stress was generated within the cell culture media by adding hydrogen peroxide to a final concentration of 0.2 μM which produces oxygen radicals.[26] For the CSP cells without the silica hydrogel shell, the viability decreased significantly by 50% after treatment with hydrogen peroxide (Figure 6b). On the other hand, the cells coated with silica hydrogel were significantly protected against the oxidative stress; there was only 8% decrease in the viability. This result demonstrated that the silica hydrogel shell on the cell-seeded GelMA microgel core was highly efficient as a protective layer against oxidative stress, by preventing the harmful reactive oxidation species from directly contacting the cells.

Degradation of Silica Hydrogel Shell. After delivery into the target site, the protective silica shell on the cell-seeded microgels needs to be degraded, in order for the cells to migrate and proliferate into the target tissue. Silica hydrogels have been shown to degrade under physiological conditions, in which SiO_2-bonded polymeric macrostructures undergo hydrolysis, and the degradation product, silicic acid, becomes solubilized.[41,42] Therefore, to monitor the degradation process, the amount of silicic acid released from the silica hydrogel coated GelMA microgels was analyzed using a colorimetric assay involving the formation of silicomolybate.[27,28] Silicic acid readily forms a complex with molybdic acid (silicomolybdate), which has the characteristic absorbance at 400 nm. The plot of absorbance at 400 nm (A_{400}) versus time shows that the amount of silicic acid increased over time, therefore confirming the degradation of silica hydrogel (Figure 7a). The plot was well fitted with eq 3, demonstrating that the degradation of silica hydrogel followed first-order kinetics.

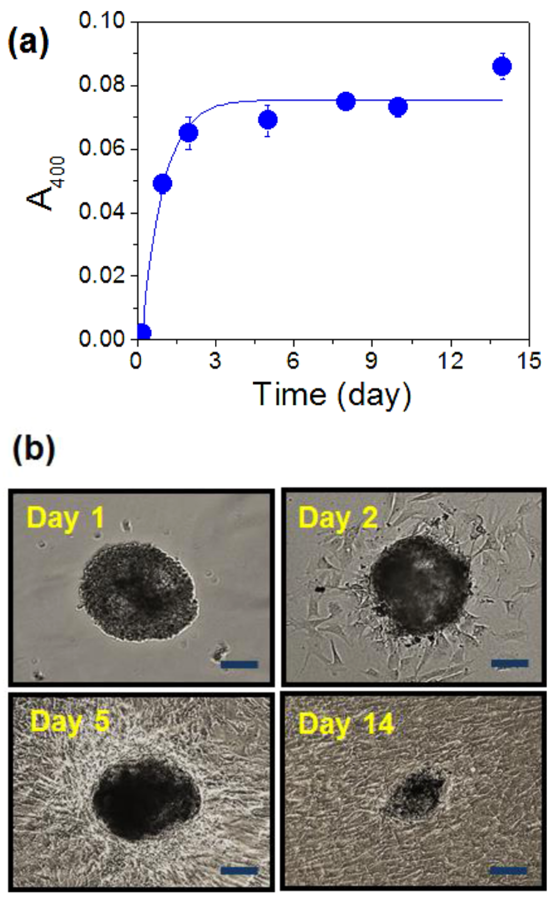

Figure 7. (a) Degradation product, silicic acid, from silica hydrogel was monitored by measuring the absorbance of silicomolybdate complex at 400 nm (A_{400}). The plot was fitted with a first-order degradation kinetics model. (b) Silica-coated CSP cell-seeded microgels were placed on a cell adhesive surface, and monitored their adhesion and proliferation over time. (Scale bar: 50 μm).

We further explored the effect of silica hydrogel shell on the cellular activity, by placing the cell-seeded core−shell microgels on the tissue-culture treated plastic surface, and monitoring the cellular migration, as similarly done in Figure 4 (Figure 7b). The cell-seeded GelMA microgels with silica shell only began to adhere to the tissue-culture treated plastic surface after two days, suggesting that a certain amount of silica hydrogel shell must be degraded in order for the cell to become exposed and adhere to the tissue-culture surface. Then, the cells were able to migrate from the microgel periphery and proliferate over time. However, it took over two weeks for the spherical structure to completely disappear, which was much longer as compared with those without the silica shell, as shown in Figure 4, suggesting that extensive degradation of the silica hydrogel was needed for the cells to be completely released from the microgels and degrade the GelMA microgels. Nevertheless, the migratory and proliferative capacities of CSP cells on GelMA microgels were not hampered by the presence of the silica hydrogel layer.

■ CONCLUSION

Taken together, this study demonstrated a facile and efficient approach for the generation of microgels as an in vitro cell culture platform to engineer injectable tissue constructs by utilizing the microfluidic flow-focusing device coupled with photopolymerization process. The monodisperse droplets consisting of photo-cross-linkable gelatin (GelMA) pregel solution generated by the microfluidic device were immediately photo-cross-linked with UV light to form GelMA microgels. The size of the microgels was readily controlled by changing the flow rates of the aqueous and oil phases. The resulting GelMA microgels provided suitable cellular microenvironment, as indicated by adhesion and proliferation of CSP cells on the microgel surface. These cells on the microgels were also able to migrate and spread onto their cell-conductive surrounding, which demonstrated that the cell-seeded GelMA microgels could be successfully used as injectable tissue constructs. Furthermore, a thin silica hydrogel was coated on the surface of the cell-seeded microgels via sol−gel method as a protective shell. The silica hydrogel shell not only effectively protected the cells from hydrogen peroxide-induced oxidative stress, but also degraded over time without affecting the cellular activities. Overall, we expect that the microfluidic approach to engineer cell-seeded microgel core combined with protective silica hydrogel shell will be a highly promising platform to engineer injectable tissue constructs for various applications in regenerative medicine.

■ ASSOCIATED CONTENT

Supporting Information

Supporting figures associated with this article. This material is available free of charge via the Internet at http://pubs.acs.org.

■ AUTHOR INFORMATION

Corresponding Author

*E-mail: alik@rics.bwh.harvard.edu.

Author Contributions

†These authors contributed equally (C.C. and J.O.).

Notes

The authors declare no competing financial interest.

■ ACKNOWLEDGMENTS

This work was supported by the Office of Naval Research Young National Investigator Award, the Presidential Early Career Award for Scientists and Engineers (PECASE), the National Science Foundation CAREER Award (DMR 0847287), and the National Institutes of Health (HL092836, DE019024, EB012597, AR057837, DE021468, EB008392, HL099073).

■ REFERENCES

(1) Hoffman, A. S. *Adv. Drug Delivery Rev.* **2002**, *54*, 3−12.
(2) Drury, J. L.; Mooney, D. J. *Biomaterials* **2003**, *24*, 4337−4351.
(3) Peppas, N. A.; Hilt, J. Z.; Khademhosseini, A.; Langer, R. *Adv. Mater.* **2006**, *18*, 1345−1360.
(4) Burdick, J. A.; Anseth, K. S. *Biomaterials* **2002**, *23*, 4315−4323.
(5) Seliktar, D.; Zisch, A. H.; Lutolf, M. P.; Wrana, J. L.; Hubbell, J. A. *J. Biomed. Mater. Res., Part A* **2004**, *68*, 704−716.
(6) Khademhosseini, A.; Langer, R. *Biomaterials* **2007**, *28*, 5087−5092.

(7) Zorlutuna, P.; Annabi, N.; Camci-Unal, G.; Nikkhah, M.; Cha, J. M.; Nichol, J. W.; Manbachi, A.; Bae, H.; Chen, S.; Khademhosseini, A. *Adv. Mater.* **2012**, *24*, 1782−1804.
(8) Tumarkin, E.; Kumacheva, E. *Chem. Soc. Rev.* **2009**, *38*, 2161−2168.
(9) Serra, C. A.; Chang, Z. *Chem. Eng. Technol.* **2008**, *31*, 1099−1115.
(10) Shah, R. K.; Shum, H. C.; Rowat, A. C.; Lee, D.; Agresti, J. J.; Utada, A. S.; Chu, L.-Y.; Kim, J.-W.; Fernandez-Nieves, A.; Martinez, C. J.; Weitz, D. A. *Mater. Today* **2008**, *11*, 18−27.
(11) Avnir, D.; Coradin, T.; Lev, O.; Livage, J. *J. Mater. Chem.* **2006**, *16*, 1013−1030.
(12) Gill, I.; Ballesteros, A. *Trends Biotechnol.* **2000**, *18*, 282−296.
(13) Nichol, J. W.; Koshy, S. T.; Bae, H.; Hwang, C. M.; Yamanlar, S.; Khademhosseini, A. *Biomaterials* **2010**, *31*, 5536−5544.
(14) Hutson, C. B.; Nichol, J. W.; Aubin, H.; Bae, H.; Yamanlar, S.; Al-Haque, S.; Koshy, S. T.; Khademhosseini, A. *Tissue Eng., Part A* **2011**, *17*, 1713−1723.
(15) Chen, Y.-C.; Lin, R.-Z.; Qi, H.; Yang, Y.; Bae, H.; Melero-Martin, J. M.; Khademhosseini, A. *Adv. Funct. Mater.* **2012**, *22*, 2027−2039.
(16) Ramon-Azcon, J.; Ahadian, S.; Obregon, R.; Camci-Unal, G.; Ostrovidov, S.; Hosseini, V.; Kaji, H.; Ino, K.; Shiku, H.; Khademhosseini, A.; Matsue, T. *Lab Chip* **2012**, *12*, 2959−2969.
(17) Oyama, T.; Nagai, T.; Wada, H.; Naito, A. T.; Matsuura, K.; Iwanaga, K.; Takahashi, T.; Goto, M.; Mikami, Y.; Yasuda, N.; Akazawa, H.; Uezumi, A.; Takeda, S. i.; Komuro, I. *J. Cell Biol.* **2007**, *176*, 329−341.
(18) Unno, K.; Jain, M.; Liao, R. *Circ. Res.* **2012**, *110*, 1355−1363.
(19) McDonald, J. C.; Whitesides, G. M. *Acc. Chem. Res.* **2002**, *35*, 491−499.
(20) Qin, D.; Xia, Y.; Whitesides, G. M. *Nat. Protoc.* **2010**, *5*, 491−502.
(21) Wang, X.; Shah, A. A.; Campbell, R. B.; Wan, K.-t. *Appl. Phys. Lett.* **2010**, *97*, 263703−263703−3.
(22) Cleveland, J. P.; Manne, S.; Bocek, D.; Hansma, P. K. *Rev. Sci. Instrum.* **1993**, *64*, 403−405.
(23) Hashmi, S. M.; Dufresne, E. R. *Soft Matter* **2009**, *5*, 3682−3688.
(24) Pfister, O.; Oikonomopoulos, A.; Sereti, K.-I.; Liao, R., Isolation of resident cardiac progenitor cells by Hoechst 33342 staining. In *Stem Cells for Myocardial Regeneration*; Lee, R. J., Ed.; Humana Press: New York, 2010; Vol. *660*, pp 53−63.
(25) Schmidt, J. J.; Jeong, J.; Kong, H. *Tissue Eng., Part A* **2011**, *7*, 2687−2694.
(26) Janero, D. R.; Hreniuk, D.; Sharif, H. M. *J. Cell. Physiol.* **1991**, *149*, 347−364.
(27) Alexander, G. B.; Heston, W. M.; Iler, R. K. *J. Phys. Chem.* **1954**, *58*, 453−455.
(28) Coradin, T.; Eglin, D.; Livage, J. *Spectroscopy* **2004**, *18*, 567−576.
(29) Kong, H. J.; Kaigler, D.; Kim, K.; Mooney, D. J. *Biomacromolecules* **2004**, *5*, 1720−1727.
(30) Cha, C.; Kohman, R. H.; Kong, H. *Adv. Funct. Mater.* **2009**, *19*, 3056−3062.
(31) Annabi, N.; Selimovic, S.; Cox, J. P. A.; Ribas, J.; Afshar Bakooshli, M.; Heintze, D.; Weiss, A.; Cropek, D. M.; Khademhosseini, A. *Lab Chip* **2013**, *13*, 3569−3577.
(32) Xu, S.; Nie, Z.; Seo, M.; Lewis, P.; Kumacheva, E.; Stone, H. A.; Garstecki, P.; Weibel, D. B.; Gitlin, I.; Whitesides, G. M. *Angew. Chem., Int. Ed.* **2005**, *44*, 724−728.
(33) Laflamme, M. A.; Murry, C. E. *Nat. Biotechnol.* **2005**, *23*, 845−856.
(34) Müller-Ehmsen, J.; Whittaker, P.; Kloner, R. A.; Dow, J. S.; Sakoda, T.; Long, T. I.; Laird, P. W.; Kedes, L. *J. Mol. Cell. Cardiol.* **2002**, *34*, 107−116.
(35) Zhang, M.; Methot, D.; Poppa, V.; Fujio, Y.; Walsh, K.; Murry, C. E. *J. Mol. Cell. Cardiol.* **2001**, *33*, 907−921.
(36) Carturan, G.; Dal Toso, R.; Boninsegna, S.; Dal Monte, R. *J. Mater. Chem.* **2004**, *14*, 2087−2098.
(37) Inama, L.; Diré, S.; Carturan, G.; Cavazza, A. *J. Biotechnol.* **1993**, *30*, 197−210.
(38) Urabe, Y.; Shiomi, T.; Itoh, T.; Kawai, A.; Tsunoda, T.; Mizukami, F.; Sakaguchi, K. *ChemBioChem* **2007**, *8*, 668−674.
(39) Muraca, M.; Vilei, M. T.; Zanusso, G. E.; Ferraresso, C.; Boninsegna, S.; Dal Monte, R.; Carraro, P.; Carturan, G. *Artif. Organs* **2002**, *26*, 664−669.
(40) Viitala, R.; Jokinen, M.; Tuusa, S.; Rosenholm, J.; Jalonen, H. *J. Sol-Gel Sci. Technol.* **2005**, *36*, 147−156.
(41) Nieto, A.; Areva, S.; Wilson, T.; Viitala, R.; Vallet-Regi, M. *Acta Biomater.* **2009**, *5*, 3478−3487.
(42) Yagüe, C.; Moros, M.; Grazú, V.; Arruebo, M.; Santamaría, J. *Chem. Eng. J.* **2008**, *137*, 45−53.